Addition of regiorandom poly(3-hexylthiophene) to solution processed poly(3-hexylthiophene):[6,6]-phenyl-C61-butyric acid methyl ester graded bilayers to tune the vertical concentration gradient

Varun Vohra, Koichi Higashimine, Tatsuya Murakami, and Hideyuki Murata

Citation: Appl. Phys. Lett. **101**, 173301 (2012); doi: 10.1063/1.4761998
View online: http://dx.doi.org/10.1063/1.4761998
View Table of Contents: http://apl.aip.org/resource/1/APPLAB/v101/i17
Published by the American Institute of Physics.

Addition of regiorandom poly(3-hexylthiophene) to solution processed poly(3-hexylthiophene):[6,6]-phenyl-C61-butyric acid methyl ester graded bilayers to tune the vertical concentration gradient

Varun Vohra,[1,a)] Koichi Higashimine,[2] Tatsuya Murakami,[2] and Hideyuki Murata[1,a)]
[1]*School of Materials Science, Japan Advanced Institute of Science and Technology, Nomi 923-1211, Japan*
[2]*Center for Nano Materials and Technology, Japan Advanced Institute of Science and Technology, Nomi 923-1211, Japan*

(Received 24 July 2012; accepted 8 October 2012; published online 22 October 2012)

Donor-acceptor vertical concentration gradient in the active layer is of crucial importance in graded bilayer poly(3-hexylthiophene):[6,6]-phenyl-C61-butyric acid methyl ester (P3HT:PCBM) solar cells. We demonstrate that upon addition of regiorandom P3HT to graded regioregular P3HT:PCBM bilayers, we are able to tune the vertical concentration gradient. With the help of energy-dispersive x-ray spectroscopy elemental mapping of the device cross-sections, we find a strong relationship between the concentration gradient profile and the device performances. Upon addition of regiorandom P3HT, the devices exhibit power conversion efficiencies up to 3.83% (compare to 3.09% for regioregular P3HT devices). © *2012 American Institute of Physics*. [http://dx.doi.org/10.1063/1.4761998]

Recent research in solution processed active layers for polymer photovoltaics demonstrated that graded bilayer (GB) solar cells represent a valuable alternative to bulk heterojunction (BHJ) solar cells.[1–3] Consecutive deposition of poly(3-hexylthiophene) (P3HT) from chlorobenzene or dichlorobenzene and [6,6]-phenyl-C61-butyric acid methyl ester (PCBM) from dichloromethane allows for the PCBM molecules to diffuse through the P3HT network while avoiding complete dissolution of the bottom P3HT layer. Theoretically, such approach will naturally create a donor-acceptor concentration gradient within the active layer of the device leading to efficient charge collection such as the one observed when introducing buffer layers of either P3HT or PCBM.[4,5] We recently reported the positive effect of improved vertical concentration gradient obtained by using rubbing technique on photovoltaic performances.[6] However, with rubbing, we cannot control the dimensions of the different layers composing the active layer. Tuning the dimensions of the different layers, namely, P3HT, intermixed, and PCBM layers, is a key parameter to make the GB attractive for both fundamental and commercial applications.

P3HT crystallinity, and consequently its molecular weight and regioregularity, highly influence both its hole transport properties and miscibility with PCBM.[7–10] Therefore, the device performances of P3HT based solar cells greatly depend on these parameters and P3HT should be carefully chosen to obtain the highest performances. More specifically, in the case of GB, the less crystalline regiorandom P3HT (RRa-P3HT) has the ability to mix better with PCBM,[9] whereas regioregular P3HT (RR-P3HT) has better transport properties.[9]

In the present communication, we focus on mixing a low molecular weight RR-P3HT with various amounts of RRa-P3HT and prepare GB based on these thin films. Energy-dispersive x-ray spectroscopy (EDS) elemental mapping provides a powerful technique to observe the morphological evolution of the active layer and relate them to the device performances upon addition of RRa-P3HT. We demonstrate that by adding RRa-P3HT, we can tune the dimensions of the different layers to achieve higher device performances with average power conversion efficiencies (PCE) reaching up to 3.83%, thus, largely overcoming those of regular devices prepared in our laboratory (average of 3.09%) as well as the record graded bilayers in literature[2,3] (average of 3.5%), and comparable to the recent results obtained with rubbed devices[6] (average of 3.81%) confirming the need for optimized concentration profiles in GB structures.

Regioregularity of P3HT not only influences the charge transport properties but also the quantity of light absorption.[7] However, a better molecular mixing of PCBM with the amorphous RRa-P3HT as compared to RR-P3HT is expected.[10] Furthermore, we have observed that RRa-P3HT is much more soluble in dichloromethane than RR-P3HT at room temperature. Therefore, we first investigate the changes in optical properties of the thin films of P3HT before and after deposition of the PCBM layer from dichloromethane. The weight concentrations (wt. % of RRa-P3HT to the total weight of P3HT which is kept unchanged) used for the experiments were 0, 5, 10, 15, 20, 25, and 50 wt. % of RRa-P3HT, and all spin-coated under the same conditions (30 mg/ml in chlorobenzene, 2500 rpm for 30 s). We note that the differences in thickness (measured with a Nanoscale Hybrid Microscope VN-8000 from Keyence across a scratch on the films) of the spin coated layers up to 20 wt. % of added RRa-P3HT are minor (approximately 80 nm thick films) and that the 25 wt. % and 50 wt. % films are, respectively, 100 and 115 nm thick. Figure 1 displays the changes observed for the absorption upon addition of RRa-P3HT to the RR-P3HT solution. The absorption measurements were carried out using a UV/Vis Spectrometer (Jasco V670).

Upon addition of RRa-P3HT, we clearly observe a blue shift and a decrease of the absorption associated with a more amorphous material. This decrease in absorption upon addition of RRa-P3HT is due to its smaller absorption coefficient

[a)]Authors to whom correspondence should be addressed. Electronic addresses: varunvohra1984@gmail.com and murata-h@jaist.ac.jp.

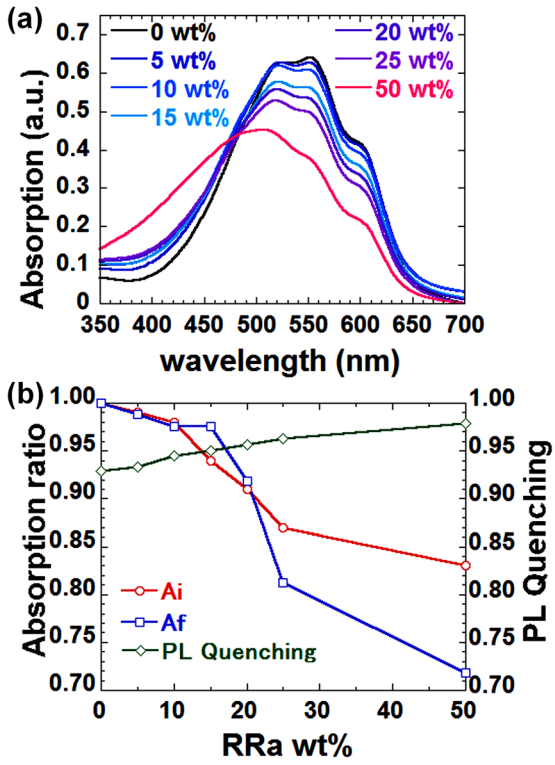

FIG. 1. Evolution of (a) the absorption spectra of thin P3HT layers obtained from RR-P3HT with increasing additional amount of RRa-P3HT ranging from 0 to 50 wt. % and (b) of A_i, A_f, and PL quenching with increasing RRa-P3HT concentration.

compared with that of RR-P3HT. To characterize the decrease in absorption, we employ the absorption ratio between the integrated absorption of the film with X wt. % of RRa-P3HT over the integration of the film of pure RR-P3HT which we define as A_i. Figure 1 displays the evolution of the values obtained for A_i with increasing RRa-P3HT wt. %. We note that the 25 and 50 wt. % films display a remarkable decrease in absorption even though thicker spin-coated films are obtained.

To fabricate the graded bilayer structure, the acceptor molecule solution (PCBM in dichloromethane, 10 mg/ml) is spin-coated on top of the P3HT layers at 4000 rpm for 10 s. The difference in solubility of RR-P3HT and RRa-P3HT in dichloromethane may lead to remarkable changes during this PCBM spin-coating step. By integrating the absorption resulting from P3HT before and after spin-coating PCBM, we obtain useful information about the reduction of the film thickness in the process. For each sample (X wt. % of RRa-P3HT), we define A_f (X wt. %) as the ratio between the integration of the absorption of P3HT after and before deposition of the PCBM layer (Figure 1). All values of A_f (X wt. %) are normalized with A_f (0 wt. %) for direct comparison with the reference sample (no additional RRa-P3HT). Increasing RRa-P3HT concentration leads to a decrease of A_f with different behaviors for concentrations up to 15–20 wt. % and above 20 wt. % of RRa-P3HT. We also note that the pure RR-P3HT film absorption is reduced upon spin-coating PCBM which suggests that, unlike what has been previously stated in literature,[2,11] a small amount of P3HT is dissolved during the spin-coating of the top PCBM layer. Finally, we use photoluminescence (PL) quenching measurements to characterize the molecular mixing between P3HT and PCBM which gradually increases upon RRa-P3HT addition. When donor and acceptor materials are in intimate contact, the electron on the LUMO of the donor falls onto the LUMO of the acceptor, resulting in a quenching of the radiative emission from the donor. PL quenching is related to the ratio between the integration of PL of the various P3HT films after (PL_f) and before (PL_i) deposition of the PCBM layer. PL_f is obtained by diving the PL resulting from the films after PCBM deposition by A_f (correction factor for the amount of P3HT dissolved in the process) and we define PL quenching as 1-(PL_f/PL_i). PL measurements were performed using a Spectrofluorometer obtained from JASCO Corporation (FP-6500) with an excitation wavelength of 550 nm. In thin films based on pure RR-P3HT, the PL quenching already displays values of around 93%. With increasing RRa-P3HT content, this value gradually increases to about 98% which confirms the improved mixing of PCBM with RRa-P3HT at the molecular level.

The more intimate molecular mixing of RRa-P3HT and PCBM increases the probability of charge generation per absorbed photon. However, the decrease in absorption and in the charge transport properties associated with the amorphous P3HT may lead to a lower short-circuit current density (J_{sc}). Table I summarizes the device characteristics obtained with increasing RRa-P3HT content. Figure 2 displays the corresponding current density-voltage (*J-V*) curves of the devices under AM 1.5.

To understand the effect of RRa-P3HT addition on the J_{sc} independently of the decrease in absorption observed previously, we introduce a corrected J_{sc}, which corresponds to the J_{sc} normalized by using the two absorption ratios of A_i and A_f in Figure1(b). The first correction factor is related to the changes in the absorption spectra and intensity when introducing RRa-P3HT, while the latter corresponds to the changes in amounts of P3HT dissolved during the deposition

TABLE I. Photovoltaic properties of devices vs additional RRa-P3HT wt. %.

RRa-P3HT (wt. %)	J_{sc} (mA/cm^2)	Corrected *Jsc*	V_{oc} (mV)	*FF* (%)	PCE (%)	R_s (Ω/cm^2)	R_{sh} (MΩ/cm^2)
0	10.05	10.05	594	51.8	3.09	4.22	0.74
5	9.49	9.70	599	54.0	3.08	2.17	0.73
10	9.93	10.37	605	57.0	3.42	1.81	0.65
15	10.34	11.26	617	60.1	3.83	1.81	0.64
20	9.40	11.26	621	59.6	3.48	2.41	0.64
25	7.45	10.55	632	44.9	2.12	7.80	0.60
50	1.72	2.89	546	20.5	0.19	28.17	0.53

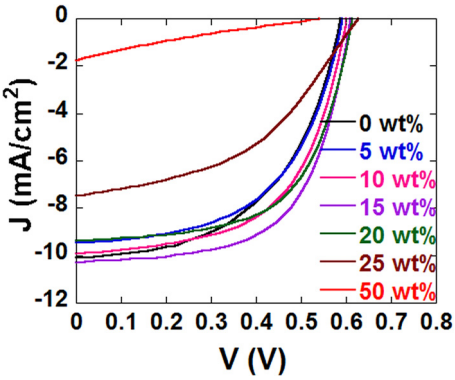

FIG. 2. J-V curves of devices with increasing wt. % of RRa-P3HT.

of the top PCBM layer. We note that the only parameter corrected by the absorption in Table I is J_{sc}. All other parameters, including PCE, correspond to the measured values. The devices obtained with additional RRa-P3HT exhibit an increase in PCE up to 3.83% (obtained for 15 wt. % of RRa-P3HT). In the 25 and 50 wt. % devices, a relatively large amount of the P3HT film is dissolved during the PCBM spin-coating process (as previously observed in Figure 1). We therefore meticulously analyze the trends observed for the device characteristics with a particular focus on understanding the evolution up to 20 wt. % of RRa-P3HT.

The open-circuit voltage (V_{oc}) displays a constant increase up to 25 wt. % of RRa-P3HT and then falls when 50 wt. % is reached. Previous results found in literature demonstrate that the V_{oc} of P3HT:PCBM devices are closely related to the crystallinity of P3HT.[12] In fact, the more amorphous RRa-P3HT has a much lower HOMO level compared to RR-P3HT, thus, leading to a wider $HOMO_{donor}$–$LUMO_{acceptor}$ gap, one of the main parameters which influences V_{oc}. The V_{oc} increase therefore results directly from a widening of the $HOMO_{donor}$–$LUMO_{acceptor}$ gap upon addition of RRa-P3HT up to 25 wt. %. The device obtained with 50 wt. % of RRa-P3HT displays a very high series resistance (R_s) resulting in a decrease of the V_{oc}. R_s, which characterizes the internal resistance of the device, is not only related to the intrinsic charge transport properties of the donor and acceptor materials but also to the vertical concentration gradient within the active layers of the devices. To have a better understanding of the trends in device parameters such as corrected J_{sc}, fill factor (FF) and R_s, the vertical concentration gradient of the devices is a key parameter. Through EDS elemental mapping, we analyze the P3HT contents through the cross-section of the devices. EDS for elemental analysis was carried out with a scanning transmission electron microscope, JEM-ARM200F from JEOL. The acceleration voltage and probe current were 200 kV and 59 pA, respectively, to obtain 256×256 pixels images with a dwell time of 1 ms/pixel. Each image was accumulated 50 times to improve the signal to noise ratio. Figure 3 displays the EDS images obtained with increasing amount of RRa-P3HT up to 25 wt. %. The corrected J_{sc} (Table I) displays a small initial decrease at 5 wt. % of RRa-P3HT followed by an increase up to 20 wt. % of added RRa-P3HT. As previously mentioned, this increase confirms that we have more intimate mixing between PCBM and RRa-P3HT as compared to RR-P3HT. However, J_{sc} depends on both charge generation and collection. Therefore, the charge transport and collection properties need to be taken into account which may explain the limit of the corrected J_{sc} at 20 wt. % of RRa-P3HT.

From Figure 3, we first note that in the 0 wt. % device, P3HT is found not only close to the PEDOT:PSS layer but also in contact with the aluminum electrode: a higher PCBM concentration layer is sandwiched between two high P3HT content layers, and therefore, electrons generated cannot percolate easily leading to an increase of R_s and a consequent decrease of the FF. This thin layer gradually disappears upon addition of RRa-P3HT up to 20 wt. %, thus, creating an ideal concentration gradient with mainly PCBM in contact with aluminum and P3HT in contact with PEDOT:PSS. Therefore, an increase of the FF and a decrease of the R_s can be observed with the electron blocking layer gradually disappearing. Moreover, this results in the formation of a PCBM buffer layer with a thickness varying from approximately 10

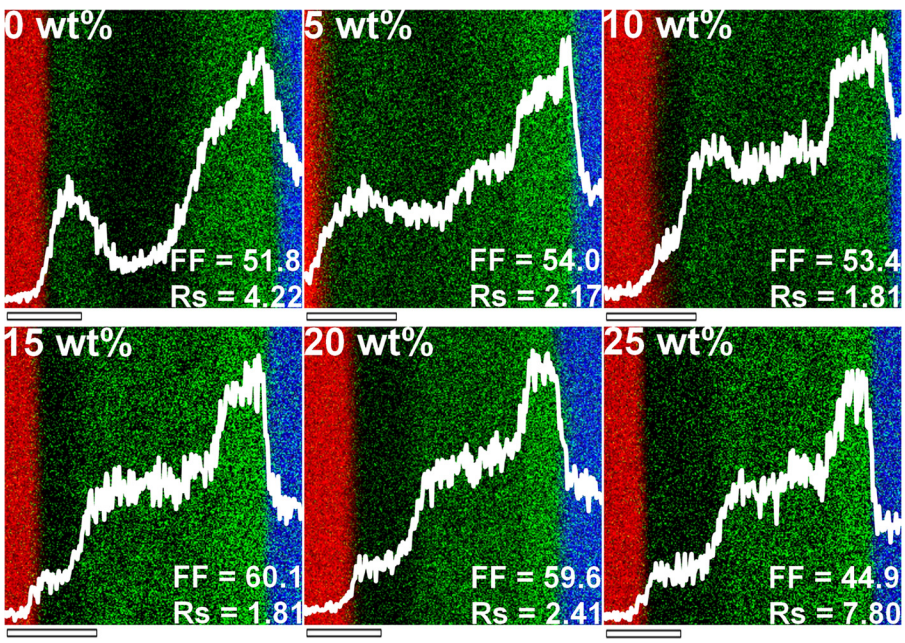

FIG. 3. Evolution of the vertical concentration gradient in the cross-section of the devices with increasing RRa-P3HT content obtained from EDS elemental mapping. EDS images display location of aluminum (red), sulfur (green), and indium (blue) with overlapped sulfur concentration gradient along the device cross-section (white line). Scale bar: 50 nm.

to 20 and finally 30 nm for the devices with 10, 15, and 20 wt. % of RRa-P3HT, respectively. As charges are generated where the donor material is in contact with the acceptor, a thick buffer layer commonly results in a increase in R_s such as the one observed when going from 15 to 20 wt. % of RRa-P3HT. The evolution of the *FF* is closely related to R_s. However, the small differences in trends may also result from the formation of a PCBM concentration gradient within the highly concentrated P3HT layer (e.g., in the 15 and 20 RRa-P3HT wt. % devices). Furthermore, we do not have information about the charge recombination rate in these devices which may also explain the deviations observed in the trends. When increasing the RRa-P3HT wt. % over 20%, a large amount of P3HT is dissolved in the process and the resulting active layers exhibit a bulk heterojunction-like morphology where both P3HT and PCBM gradually spread throughout the whole active layer thickness. The high R_s obtained for the devices with 25 and 50 wt. % of RRa-P3HT is most probably related to the intrinsic hole transport properties of the amorphous RRa-P3HT causing the decrease of the *FF* and consequently, the PCE.

In summary, we demonstrate that the addition of RRa-P3HT to GB P3HT:PCBM solar cells displays various positive effects when choosing the adequate amount of amorphous material added. Up to 15 wt. % of additional RRa-P3HT, we observe an improvement of all photovoltaic characteristics. The increase in corrected J_{sc} can be attributed to the more intimate molecular mixing of PCBM with the amorphous P3HT while the V_{oc} increase is related to the intrinsic properties of RRa-P3HT (stabilized HOMO level as compared to RR-P3HT leading to a wider donor-acceptor HOMO-LUMO gap). EDS elemental mapping of the device cross-sections demonstrate that upon addition of RRa-P3HT, we control the vertical concentration gradient of P3HT:PCBM within the active layer and are therefore able to reduce the R_s leading to a notable increase of the *FF* (from 51.8% up to 60.1%). The highest PCE obtained for devices containing 15 wt. % of RRa-P3HT is 3.83% in average bringing these devices among the best performing graded bilayer solar cells.

The work was supported by a Grant-in-Aid for Scientific Research on Innovative Areas (No. 20108012, "pi-Space") from the Ministry of Education, Culture, Sports, Science, and Technology, Japan. V. Vohra would like to greatly acknowledge financial support through research fellowships from the Japan Society for Promotion of Science for post-doctoral fellowships for foreign researchers.

[1]D. H. Wang, H. K. Lee, D.-G. Choi, J. H. Park, and O. O. Park, Appl. Phys. Lett. **95**, 043505 (2009).
[2]A. L. Ayzner, C. J. Tassone, S. H. Tolbert, and B. J. Schwartz, J. Phys. Chem. C **113**, 20050–20060 (2009).
[3]K. H. Lee, P. E. Schwenn, A. R. G. Smith, H. Cavaye, P. E. Shaw, M. James, K. B. Krueger, I. R. Gentle, P. Meredith, and P. Burn, Adv. Mater. **23**, 766–770 (2011).
[4]C.-W. Liang, W.-F. Su, and L. Wang, Appl. Phys. Lett. **95**, 133303 (2009).
[5]B. Tremolet de Villers, C. J. Tassone, S. H. Tolbert, and B. J. Schwartz, J. Phys. Chem. C **113**, 18978–18982 (2009).
[6]V. Vohra, G. Arrighetti, L. Barba, K. Higashimine, W. Porzio, and H. Murata, J. Phys. Chem. Lett. **3**(13), 1820–1823 (2012).
[7]R. Mauer, M. Kastler, and F. Laquai, Adv. Funct. Mater. **20**, 2085–2092 (2010).
[8]A. M. Ballantyne, L. Chen, J. Dane, T. Hammant, F. M. Braun, M. Heeney, W. Duffy, I. McCulloch, D. D. C. Bradley, and J. Nelson, Adv. Funct. Mater. **18**, 2373–2380 (2008).
[9]C. Goh, R. J. Kline, M. D. McGeheea, E. N. Kadnikova, and J. M. J. Fréchet, Appl. Phys. Lett. **86**, 122110 (2005).
[10]M. Campoy-Quiles, Y. Kanai, A. El-Basaty, H. Sakai, and H. Murata, Org. Electron. **10**, 1120–1132 (2009).
[11]C. W. Rochester, S. A. Mauger, and A. J. Moulé, J. Phys. Chem. C **16**, 7287–7292 (2012).
[12]W. C. Tsoi, S. J. Spencer, L. Yang, A. M. Ballantyne, P. G. Nicholson, A. Turnbull, A. G. Shard, C. E. Murphy, D. D. C. Bradley, J. Nelson, and J.-S. Kim, Macromolecules **44**, 2944–2952 (2011).